NIH Public Access
Author Manuscript
Cell Metab. Author manuscript; available in PMC 2015 January 07.

Published in final edited form as:
Cell Metab. 2014 January 7; 19(1): 84–95. doi:10.1016/j.cmet.2013.11.018.

Regulation of steatohepatitis and PPARγ signaling by distinct AP-1 dimers

Sebastian C. Hasenfuss[1,2], **Latifa Bakiri**[1], **Martin K. Thomsen**[1], **Evan G. Williams**[3], **Johan Auwerx**[3], and **Erwin F. Wagner**[1]

[1]Genes, Development and Disease Group, F-BBVA Cancer Cell Biology Programme, National Cancer Research Centre (CNIO), 28029 Madrid, Spain. [2]University of Freiburg, Faculty Biology, 79104Freiburg, Germany. [3]Laboratory of Integrative and Systems Physiology, School of Life Sciences, École Polytechnique Fédérale, 1015 Lausanne, Switzerland.

Summary

Non-alcoholic fatty liver disease (NAFLD) affects up to 30% of the adult population in Western societies, yet the underlying molecular pathways remain poorly understood. Here, we identify the dimeric Activator Protein 1 as a regulator of NAFLD. The Fos-related antigen 1 (Fra-1) and 2 (Fra-2) prevent dietary NAFLD by inhibiting pro-steatotic PPARγ signaling. Moreover, established NAFLD and the associated liver damage can be efficiently reversed by hepatocyte-specific Fra-1 expression. In contrast, c-Fos promotes PPARγ expression, while c-Jun exerts opposing, dimer-dependent functions. Interestingly, JunD was found to be essential for PPARγ signaling and NAFLD development. This unique antagonistic regulation of PPARγ by distinct AP-1 dimers occurs at the transcriptional level and establishes AP-1 as a link between obesity, hepatic lipid metabolism and NAFLD.

Keywords

NAFLD; Steatosis; Activator Protein 1; PPARγ; Lipids; Transcription

Introduction

Given their high energy-to-weight ratio compared to carbohydrates and proteins, lipids are the most efficient energy substrate in mammals. The adipose tissue is the major lipid storage organ and it is essential for controlling metabolic homeostasis(Sethi and Vidal-Puig, 2007).

© 2013 Elsevier Inc. All rights reserved.

Corresponding author: Erwin F. Wagner F-BBVA Cancer Cell Biology Programme National Cancer Research Centre (CNIO), Melchor Fernandez Almagro 3, 28029 Madrid, Spain Phone: + 34 91 224 69 12 Fax: + 34 91 224 69 14 ewagner@cnio.es.

Publisher's Disclaimer: This is a PDF file of an unedited manuscript that has been accepted for publication. As a service to our customers we are providing this early version of the manuscript. The manuscript will undergo copyediting, typesetting, and review of the resulting proof before it is published in its final citable form. Please note that during the production process errors may be discovered which could affect the content, and all legal disclaimers that apply to the journal pertain.

Conflict of interest: The authors declare no conflict of interest

For procedure details, see Extended Experimental Procedures.

NIH-PA Author Manuscript
NIH-PA Author Manuscript
NIH-PA Author Manuscript

NIH-PA Author Manuscript

NIH-PA Author Manuscript

NIH-PA Author Manuscript

In the healthy state, tissues such as muscle and liver store only minor quantities of lipids(Lara-Castro and Garvey, 2008). However, metabolic stress, as occurring in obese or alcohol-abusing patients, can cause massive ectopic lipid deposition, leading to a disease state, termed “steatosis” or “fatty liver disease”. Depending on the etiology, this disease can be further subgrouped into alcoholic or non-alcoholic fatty liver disease (AFLD and NAFLD respectively). NAFLD is the most common liver disorder in industrialized countries and it frequently leads to severe liver inflammation and damage, a disease state termed “non-alcoholic steatohepatitis”(NASH)(Browning and Horton, 2004). Moreover, NAFLD contributes to hepatic insulin resistance in diabetes(Farese et al., 2012) and is a risk factor for liver dysfunction and cancer development(Smedile and Bugianesi, 2005). Understanding the cellular and molecular mechanisms leading to NAFLD, as well as the identification of novel targets for NAFLD therapy has therefore become a priority(Cohen et al., 2011; Lazo and Clark, 2008).

The Activator Protein-1 (AP-1) (Fos/Jun)protein complex is a dimeric leucine zipper(bZIP) transcription factor. Three different Jun proteins (c-Jun, JunB and JunD) and four different Fos proteins (c-Fos, FosB, Fra-1 and Fra-2) formAP-1 dimer. Jun proteins can either form homodimers, such as c-Jun/c-Jun or c-Jun/JunB, or heterodimers, such as c-Jun/c-Fos. In contrast, Fos proteins exclusively form heterodimers(Halazonetis et al., 1988). Jun and Fos proteins also form heterodimers with other bZIP transcription factors, such as specific MAF and ATF family members(Eferl and Wagner, 2003). Thus, a vast combinatorial variety of AP-1 dimers with likely different molecular and biological functions exists(Hess et al., 2004; Verde et al., 2007; Wagner et al., 2010). Studies using genetically modified mice have unravelled essential roles of AP-1-forming proteins in development, inflammation and cancer(Eferl and Wagner, 2003). Moreover, AP-1 modulates the response to acute cellular insults, such as oxidative stress and DNA damage (Shaulian and Karin, 2002). Cellular stress typically activates AP-1 by augmenting transcription, protein stability and transactivation potential of Jun and Fos family members (Wagner and Nebreda, 2009). In the liver, the genetic inactivation of single *Jun* or *Fos* genes in hepatocytes does not compromise organ homeostasis (Bakiri and Wagner, 2013; Eferl and Wagner, 2003). However, AP-1 is critical for the liver’s response to acute stress. For example, c-Jun protects hepatocytes from injury (Fuest et al., 2012; Hasselblatt et al., 2007) and is essential for liver regeneration (Behrens et al., 2002) and carcinogenesis (Eferl et al., 2003; Machida et al., 2010; Min et al., 2012). More recently, we have documented that Fra-1, but not Fra-2, protects hepatocytes from acetaminophen overdose, a paradigm for xenobiotic-mediated acute liver failure (Hasenfuss et al., 2013). In contrast, little is known about the role of AP-1 in chronic stress conditions and the potential contribution of AP-1 to the development of hepatic metabolic disease. Here we combined system genetics with gain- and loss-of-function mouse models to study the function of AP-1 in hepatic lipid metabolism and NAFLD development. We show that, depending on dimer composition, AP-1 either represses or activates the transcription of the pro-steatotic nuclear receptor Peroxisome Proliferator-Activated Receptor γ (PPARγ), which promotes hepatic lipid uptake and lipid droplet formation. Some AP-1 proteins, such as Fra-1 and Fra-2, inhibit the PPARγ pathway and reduce hepatic lipid content. In contrast, other AP-1 proteins, such as c-Fos and JunD induce hepatic PPARγ signaling and lipid accumulation. We also show that AP-1 regulates

NIH-PA Author Manuscript

NIH-PA Author Manuscript

NIH-PA Author Manuscript

the PPARγ pathway through direct regulation of the *Pparg2* promoter. Using a mouse model for inducible hepatocyte-restricted Fra-1 expression, we demonstrate that the Fra-1-induced suppression of the PPARγ pathway can revert established NAFLD. For the first time, liver-specific single chain Jun~Fos forced dimer mice were employed, in which dimerization of a Fos protein is restricted to a single Jun partner (Bakiri et al., 2002). The analyses of these mouse models provide *in vivo* evidence that distinct AP-1 dimers regulate the PPARγ pathway in an antagonistic fashion. Finally, we show that JunD is essential for efficient PPARγ signalling and NAFLD formation. Overall, this study identifies AP-1 as a link between dietary obesity, hepatic lipid metabolism and NAFLD.

Results

Fra-1/AP-1 regulates hepatic lipid metabolism and NAFLD

To identify a possible function of AP-1 in metabolism, we analyzed 42 genetically diverse mouse strains from the BXD mouse genetic reference population (GRP)(Peirce et al., 2004). 10 animals for each strain were split evenly into two cohorts fedchow diet (CD) or high-fat diet (HFD) for five months. Hepatic AP-1 mRNA expression was then analyzed using genome-wide expression profiles from the BXD strains. *Fra-1* mRNA levels were found to be significantly reduced in the HFD-fed cohort, while the expression ofc-*fos*, *fosB*, *fra-2*, *c-jun*, *junb* and *jund* were not affected by the diet(Figure 1A and FigureS1A). To explore whether *Fra-1* could causally contribute to HFD-associated metabolic changes in the liver, we analyzed hepatic metabolism in Fra-1^{hep} mice, a previously established model of Doxycycline (Dox)-controllable hepatocyte-restrictedFra-1-overexpression, which does not display any obvious phenotype under basal conditions (Hasenfuss et al., 2013)(for details on mouse strains see Table S1). After HFD feeding, the livers appeared less pale on the macroscopic level and weighed significantly lessin Fra-1^{hep} mice compared to HFD-fed littermate controls (Figure 1B, C). Liver histology indicated a reduction in lipid droplets in mutant mice (Figure 1B), which was confirmed by the quantitation of Oil-RedO (ORO)-positive lipid droplets and liver triglyceride (TG) content analysis (Figure 1C).

We next addressed the effect of Fra-1 expression on NAFLD-associated liver damage and inflammation. Augmented serum levels of the liver damage marker alanine aminotransferase (ALT) and increased hepatic inflammation marker expression was observed in controls after HFD-feeding, but not in Fra-1^{hep} mice(Figure 1C and Figure S1B). Moreover, immunohistochemistry (IHC) for the pan-lymphocyte marker CD45 and the macrophage markerF4/80 revealed a significant reduction in immune cell infiltrates in HFD-fed mutants compared to diet-matched controls (Figure S1C). In the HFD-fed state, serum IL-6 levels were also reduced in HFD-fed Fra-1^{hep} mice compared to controls (Table S2A). We next explored the effects of hepatic Fra-1 expression on circulating metabolite and hormone levels. Serum TG and cholesterol were mildly elevated in HFD-fed Fra-1^{hep}compared to control mice in the fasted and/or fed states, while other serum parameters were not affected (Table S2A,B). Despite decreased NAFLD and liver damage, glucose tolerance and insulin tolerance tests (GTT and ITT) revealed that glucose metabolism was not improved, but rather slightly worsened in HFD-fed mutants as compared to controls (Figure S1D). Similar effects of Fra-1 on NAFLD development were also observed in Fra-1^{hep} mice on a

NIH-PA Author Manuscript

NIH-PA Author Manuscript

NIH-PA Author Manuscript

C57BL/6J background or using 60% kCal/fat HFD (Table S2B and data not shown). These data collectively suggest that hepatocyte-specific Fra-1 expression protects from dietary-induced NAFLD and secondary liver damage and inflammation, but has little impact on systemic obesity and glucose metabolism.

Fra-1 represses the PPARγ pathway

We next analyzed the molecular mechanisms underlying reduced NAFLD in Fra-1^{hep} mice. Genome-wide hepatic gene expression analyses in CD- and HFD-fed Fra-1^{hep} mice demonstrated that the expression of ~3000 genes was changed by at least 1.5 fold in Fra-1^{hep} livers. The vast majority of these genes were regulated in a similar fashion in both dietary conditions and many PPARγ targets, e.g. *adipsin* and *cidea* were among the top-downregulated genes (Figure 2A). KEGG pathway analysis (Kanehisa et al., 2012) of the top 2000 most changed genes established PPARγ signaling among the most significantly affected pathways in both diet conditions (Figure 2B). A highly significant fraction of mRNAs, which were reduced in Fra-1^{hep} mice, were encoded by genes with promoters containing putative AP-1 sites (p=9.0E-13) and PPARγ response elements (PPREs) (p=3.3E-11), as revealed by UCSC TFBS conserved tracks analyses (http://david.abcc.ncifcrf.gov/)(Huang da et al., 2009) (Table S3). qRT-PCR, immunoblot and IHC analyses confirmed decreased hepatic *pparγ* mRNA/PPARγ protein expression in CD- and HFD-fed Fra-1^{hep} mice (Figure 2C,D and Figure S2A).

Decreased *pparγ* mRNA levels were due to reduced expression of *pparγ2*mRNA, the main *pparγ* isoform in the liver (Figure 2C and Figure S2D)(Lee et al., 2012). Among other metabolic regulators *Nr0b2*, a potential PPARγ target(Kim et al., 2007)and regulator(Kim et al., 2013), which encodes the orphan nuclear receptor SHP, was also found reduced in HFD-fed Fra-1^{hep} mice (Figure S2C). Moreover, we confirmed reduced mRNA expression for several PPARγ target genes, such as *fabp1* and *lpl*, involved in hepatic lipid uptake, and *plin2*, *cidea*, *fitm1*, *fitm2*, *g0s2*, involved in lipid droplet formation (Figure S2E). Notably, the Fra-1-induced reduction of *ppary2* expression was reversible, as *pparγ2* levels reverted to baseline levels upon switching off the transgene (Figure S2F). Kinetic analyses of another inducible Fra-1 mouse model (Fra-1^{tetON} mice)(Hasenfuss et al., 2013) revealed that hepatic *pparγ2* mRNA decreased as early as 4 days after Fra-1 induction (Figure S2G).

Adenoviral PPARγ delivery restores NAFLD/steatosis in Fra-1^{hep} mice

Gain- and loss-of-function studies previously established that hepatocyte PPARγ is both essential and sufficient for NAFLD formation (Gavrilova et al., 2003; Lee et al., 2012; Matsusue et al., 2003; Matsusue et al., 2008; Medina-Gomez et al., 2007; Moran-Salvador et al., 2011). To determine whether reduced NAFLD development in Fra-1^{hep} mice is directly due to decreased PPARγ levels, HFD-fed Fra-1^{hep} and control mice were intravenously injected with either Adeno-PPARγ or Adeno-GFP control virus 8-10 days prior to sacrifice. Adeno-PPARγ did not have any obvious effect on liver macroscopy in steatotic control mice (Figure 3A). In contrast, PPARγ expression increased ORO-positive lipid droplets, liver TG content, and liver/body weight ratio in HFD-fed Fra-1^{hep} mutant mice (Figure3A,B). Moreover, Adeno-PPARγ increased PPARγ target gene expression in the livers of Fra-1^{hep} mice, as compared to Adeno-GFP treated mutants (Figure 3C,D). These

NIH-PA Author Manuscript

NIH-PA Author Manuscript

NIH-PA Author Manuscript

data demonstrate that the short-term induction of PPARγ signaling restores hepatic fat accumulation in HFD-fed Fra-1^{hep} mice, supporting its central function in the hepatic phenotype of Fra-1^{hep} mutant mice.

Reversion of NAFLD by hepatocyte-specific Fra-1 expression

To examine whether Fra-1 induction in steatotic livers ameliorates disease symptoms, Fra-1^{hep}and control littermates were generated in the “Fra-1 off” state and HFD-feeding was started at 1 month of age (Figure 4A). As expected, control and mutant mice were indistinguishable at 7 months of age in the absence of transgene expression(Figure 4B-D). Immunoblot analyses confirmed comparable PPARγ, Fsp27 and Fabp1 levels between control and mutant mice in the “Fra-1 off” state (Figure 4E). A cohort of Fra-1^{hep}and control mice were kept on HFD, but Fra-1 expression was switched on in mutant mice at 7 months of age (Fra-1 off-on). After 2 months of Fra-1 induction, serum ALT was significantly lower in Fra-1^{hep} mice than in control littermates and continued to improve 3 months later, while the mice were maintained on HFD (Figure 4C). At this point the liver was collected for macroscopy, histology, ORO-quantitation, liver/body weight ratio and liver TG content analysis, revealing an almostcomplete reversion of NAFLD in Fra-1^{hep}mutants (Figure 4B-D). Immunoblotting and qRT-PCR analyses confirmed transgene induction, as well as the repression of PPARγ, targets of PPARγ and inflammatory markers after switching on Fra-1 expression (Figure 4E,F). These data suggest that the Fra-1-mediated repression of the PPARγ pathway efficiently reversed established NAFLD and liver damage in mice, even under continued stress of HFD feeding.

PPARγ links AP-1 to lipid metabolism

We next searched for correlations between AP-1 genes, PPARγ and PPARγ targets in gene expression arrays from the BXD family of wild-type inbred mouse strains. This analysis revealed that hepatic *pparγ* expression, assessed with a probe detecting both *pparγ* isoforms, is significantly upregulated in HFD-fed cohorts (Figure S3A). As expected, *pparγ* mRNA levels strongly correlated with the expression of PPARγ targets, such as *cidea* and *adipsin* (Figure S3B). Notably, and consistent with our findings in Fra-1^{hep}mice, a significant inverse correlation was found between *fra-1* and *pparγ* and *fra-1* and *cidea* regardless of the diet (Figure 5A). Other PPARγ targets, such as *adipsin* followed a similar trend without reaching statistical significance (Figure 5A). Interestingly, *junb*, a potential dimerization partner for Fra-1 also negatively correlated with *pparγ* (Figure 5B), indicating that several AP-1 proteins consistently regulate PPARγ signaling in genetically diverse populations.

Antagonistic regulation of *Pparg2* by AP-1

The proximal promoter of the mouse *Pparg2* gene (encoding PPARγ2), in which we identified several putative AP-1 sites (Figure 5C), is conserved across species (Figure S3D). Thus, we assessed the binding of various Jun and Fos proteins to the *Pparg2* promoter. Chromatin samples were prepared from liver tissue of mice deficient for individual AP-1 genes (Table S1) and their respective littermates to control for antibody specificity. Chromatin immunoprecipitation (ChIP) assays revealed that Fra-1, Fra-2, c-Fos, c-Jun, JunB

NIH-PA Author Manuscript

NIH-PA Author Manuscript

NIH-PA Author Manuscript

and JunD all efficiently bound to the proximal *Pparg2* promoter fragment in liver tissue (Figure 5D). α-Flag ChIP assays also revealed a significant enrichment for the same promoter fragment in livers from Fra-1^{hep} and c-Fos^{hep} mice (Figure S3E), a mouse model for inducible c-Fos expression in the liver (Table S1). No enrichment was observed for an unrelated genomic fragment in the same α-Flag ChIP samples (Figure S3E). Fra-1, Fra-2, c-Fos and Jun proteins also bound to the human *PPARG2* promoter, as α-Fra-1, α-Fra-2, α-c-Fos, α-pan-Jun, but not control IgG ChIP samples were enriched for the proximal *PPARG2* promoter region in human HuH7 hepatoma cells (Figure5E). These data indicate that Jun and Fos proteins are functionally involved in the direct regulation of the mouse *Pparg2*/human *PPARG2* promoter. We therefore analyzed the effects of Fos and Jun proteins on *PPARG2* promoter activity. Reporter assays revealed that the activity of a human *PPARG2* luciferase reporter was inhibited by transfecting Fra-1 and also by Fra-2 in HuH7 and 293T cells (Figure 5F and Figure S3F). In contrast, the *PPARG2* luciferase reporter was activated by c-Fos and inhibited by a dominant-negative Δc-Jun construct, which lacks a transactivation domain (Figure 5F and Figure S3F). Finally, *PPARG2* reporter activation by c-Fos was efficiently inhibited by co-transfecting increasing amounts of Fra-2 (Figure 5G). These data demonstrate that c-Fos and Fra-1/2 regulate the *PPARG2* promoter in an antagonistic manner.

AP-1 dimer-specific regulation of PPARγ signaling

The consequences of hepatic c-Fos expression were analyzed in c-Fos^{hep} mice. As early as 1 week after c-Fos induction, a strong increase in *ppary2 mRNA*, PPARγ protein and PPARγ target gene expression was observed in c-Fos^{hep} mice, while *ppary1* was only mildly affected and *nr0b2* unchanged (Figure 6A,B and Figure S4A,B). After switching off transgene expression, *c-fos*, *ppary2* and PPARγ target genes reverted to baseline levels (on-off, Figure 6A). The reversible induction of *ppary2*expression was confirmed in c-Fos^{hep} mice after 8 weeks of transgene induction (Figure S4B). Next, we studied the effect of Jun~c-Fos forced dimers(Bakiri et al., 2002) on hepatic PPARγ signaling using transgenic mice, in which dimerization of c-Fos is restricted to c-Jun, JunB or JunD (Table S1). The expression of all Jun~c-Fos dimers, such as c-Jun~c-Fos, JunB~c-Fos and JunD~c-Fos, increased *ppary2* mRNA and PPARγ target gene expression in the livers of mutant mice, with c-Jun~c-Fos causing the strongest induction (Figure 6C). As the expression of c-Fos or Jun~c-Fos forced dimers rapidly caused lethal liver dysplasia (*Bakiri et al.*, unpublished), the long-term consequences of increased PPARγ signaling on lipid metabolism and NAFLD could not be further investigated.

We next explored the effect of Fra-2 and Fra-2/AP-1 dimers on PPARγ signaling and hepatic lipid metabolism. In contrast to c-Fos and Jun~c-Fos dimers, hepatocyte-restricted Fra-2 monomer expression in Fra-2^{hep} mice inhibited the PPARγ pathway and prevented NAFLD development (Figure S4C-G). c-Jun~Fra-2 forced dimers in c-Jun~Fra-2^{hep} mice suppressed PPARγ signaling and NAFLD development to a similar extent as Fra-2 monomers(Figure 6D,E and Figure S4H-J). In contrast to most established PPARγ target genes, *nr0b2*levels were unaffected in Fra-2^{hep}mice (Figure S4G), while a mild up-regulation of *nr0b2* mRNA was observed in CD-fed c-Jun~Fra-2^{hep} mice (Figure S4J).

NIH-PA Author Manuscript

NIH-PA Author Manuscript

NIH-PA Author Manuscript

These data collectively suggest an antagonistic regulation of the PPARγ pathway and lipid metabolism by c-Fos/AP-1 and Fra-2/AP-1 dimers*in vivo*.

JunD is essential for NAFLD development

To investigate whether individual Jun or Fos members are essential for hepatic PPARγ expression and lipid metabolism, we employed loss-of-function mutant mice. Individual gene inactivation of *Fra-1*, *Fra-2* or *c-Fos* had no effect on hepatic *pparγ2* expression nor on HFD-induced NAFLD (Figure S5A and data not shown). Similarly, the single inactivation of *c-Jun* or *Junb* did not affect hepatic *pparγ2* expression (Figure S5A), while JunD$^{-/-}$ mice displayed decreased *pparγ2*levels in the liver under basal conditions (Figure S5A). We therefore analyzed HFD-induced NAFLD development in JunD-deficient mice. Liver macroscopy, histology, liver TG content analyses and ORO-quantitation revealed decreased HFD-induced NAFLD in JunD$^{-/-}$ livers (Figure 7A,B). qRT-PCR, immunoblot and IHC analysis confirmed decreased *pparγ2 mRNA*/PPARγ protein levels in HFD fed JunD$^{-/-}$ mice compared to controls in both diet conditions (Figure 7C and Figure S5B). qRT-PCR analyses revealed reduced expression of the PPARγ targets *cidea* and *fitm1*in JunD$^{-/-}$livers, whereas *nr0b2* expression was not affected (Figure S5C).

As previously reported(Thepot et al., 2000), JunD$^{-/-}$ mice had a reduced body weight and this effect was maintained in HFD (Figure7B). Total liver and fat pad weights were specifically decreased after HFD-feeding in JunD$^{-/-}$ mice compared to littermate controls (Figure 7B and Table S4). Interestingly, reduced *pparγ2* mRNA was also observed in heart tissue of HFD-fed JunD$^{-/-}$ mice (Figure S5D), indicating that AP-1 might also regulate the PPARγ pathway in other organs.

Discussion

Combined forward and reverse genetic approaches have a strong potential for discovering new regulators of metabolism. The initial identification of *Fra-1*as a potential obesity-related gene in livers from the BXD population of inbred mouse strains prompted us to further explore the role of AP-1 proteins. Subsequent mechanistic studies led to the discovery that AP-1 can function as a molecular link between obesity and liver metabolism. First, this study established AP-1 as a potent regulator of lipid metabolism and NAFLD development. Second, gene pathway analysis and BXD population genetics highlighted the AP-1 complex as a novel regulator of hepatic PPARγ signaling. Third, we demonstrate that Fra-1 repressed the PPARγ-dependent expression of genes involved in lipid uptake/lipid droplet formation, thereby efficiently improved established steatosis, liver damage and inflammation. Fourth and maybe most intriguingly, the mouse *Pparg2* and the human *PPARG2* promoter were found to be regulated in an antagonistic fashion by distinct AP-1 dimers (Figure 7D).

PPARγ promotes lipid uptake by increasing the expression of lipid transporters, such as fatty acid binding proteins (Fabps), and by promoting lipid storage in lipid droplets. Lipid droplet proteins (LDPs) inhibit TG lipolysis thereby preventing lipid-droplet breakdown (Fujimoto et al., 2008; Puri et al., 2008; Sun et al., 2012). Several LDPs are regulated by PPARγ at the transcriptional level(reviewed in Tontonoz and Spiegelman, 2008) and

NIH-PA Author Manuscript

NIH-PA Author Manuscript

NIH-PA Author Manuscript

promote NAFLD in mice, including Cidea, Plin2, and Fsp27(Chang et al., 2006; Dalen et al., 2004; Matsusue et al., 2008; Sun et al., 2012; Varela et al., 2008; Zhou et al., 2012). Similarly, deletion of the fatty acid transporter *Fabp1*reduced the dietary induction of NAFLD (Newberry et al., 2003; Newberry et al., 2006). Previous studies suggested that hepatic PPARγ also promotes hepatic lipogenesis(Matsusue et al., 2003; Medina-Gomez et al., 2007). In Fra-1^{hep} mice, which display a dramatic reduction in PPARγ levels, decreased expression of the Stearoyl-CoA desaturase-1 (SCD-1), a key enzyme in the generation of unsaturated fatty acids, was observed. However, no consistent changes in the expression of SREBP-1/2, the main transcriptional regulators of *de novo* lipogenesis, nor in the SREBP-1/2 targets FAS and ACC, were observed. Since FAS and ACC catalyze the rate-limiting steps in fatty acid synthesis, altered lipogenesis likely does not play a major role in the Fra-1-mediated repression of NAFLD. Instead, decreased hepatic lipid uptake and lipid droplet formation is most likely the primary cause for reduced steatosis formation in Fra-1^{hep}, Fra-2^{hep} and c-Jun~Fra-2^{hep} mice. Previous reports have shown that PPARγ induced the expression of *Nr0b2* (Kim et al., 2007). In line with this, HFD-fed Fra-1^{hep} mice displayed reduced *pparγ2* and *nr0b2* levels, which appeared normalized after Adeno-PPARγ treatment. More recently, *Nrob2* was shown to be required for hepatic PPARγ expression and NAFLD(Kim et al., 2013). However, we did not observe a consistent correlation between *pparγ2* and*nr0b2* expression across dietary conditions in our AP-1 mutant mouse models. Therefore, AP-1 likely regulates *pparγ2* and NAFLD independently of *Nr0b2*.

Hepatocyte-specific *Pparg* deletion, like Fra-1 overexpression, has been shown to reduce liver TG and to increase serum TG levels in the obese ob/ob mice and the AZIP lipodystrophy model, likely due to decreased hepatic lipid uptake(Gavrilova et al., 2003; Matsusue et al., 2003). Moreover, PPARγ2-dependent hepatic steatosis has been suggested to buffer systemic TG levels (Medina-Gomez et al., 2007). Similar to mice with hepatocyte-restricted *Pparg* deletion, Fra-1^{hep} mice displayed worsened glucose metabolism after HFD-feeding, despite a reduction in NAFLD. Thus, hepatic Fra-1 overexpression largely phenocopies the effects of hepatocyte-specific *Pparg*deletion on lipid and glucose metabolism. As elevated serum TG levels are associated with diabetes development, increased serum TG levels likely contribute to the deterioration of glucose metabolism in HFD-fed Fra-1^{hep} and *Pparg*-deficient mice.

Our data suggest a functional antagonism between activating c-Fos/AP-1 and repressing Fra/AP-1 dimers. Interestingly, c-Jun/c-Fos dimers increased, whereas c-Jun/Fra-2 dimers reduced PPARγ2 expression, suggesting a partner-dependent effect of c-Jun on *Pparg2* promoter activity. Previous studies in other organs suggested overlapping functions of c-Fos and Fra-1/2(Fleischmann et al., 2000; Matsuo et al., 2000). Thus, we here identify *Pparg* as the first gene to be antagonistically regulated by different Fos proteins. This finding raises the intriguing question: How do structurally similar protein complexes, such as c-Fos/AP-1 and Fra/AP-1 dimers, have opposite effects on the same promoter? While further research is required to address this question, several AP-1 co-repressors, such as Sirt1 (Purushotham et al., 2009)and HDAC3 (Feng et al., 2011; Knutson et al., 2008; Sun et al., 2012) are involved

NIH-PA Author Manuscript

NIH-PA Author Manuscript

NIH-PA Author Manuscript

in hepatic lipid metabolism. We speculate that specifically Fra/AP-1 dimers might interact with such co-repressors to inhibit *Pparg2* promoter activity.

Among Jun proteins, JunD was found to be important for NAFLD development in the liver. As $JunD^{-/-}$ mice are leaner and display reduced adiposity, the possibility that extrahepatic functions of JunD contribute to decreased NAFLD development in $JunD^{-/-}$ mice cannot be excluded. However, JunD is essential for normal *pparγ2* mRNA/PPARγ protein expression and bound to the *Pparg2* promoter in liver tissue, suggesting JunD as a novel physiologically relevant regulator of hepatic PPARγ signaling. Given the key function of PPARγ in NAFLD development, reduced PPARγ signaling in the liver likely contributes to NAFLD resistance in $JunD^{-/-}$ mice.

The described data from gain-and loss-of-function mouse models, together with the correlations between AP-1 components and the PPARγ pathway in the BXD cohort, establish AP-1 as an important regulator of PPARγsignaling and NAFLD. HFD affects a plethora of cellular signaling cascades, such as the Insulin(Kim and Kahn, 1994), the JNK(Hibi et al., 1993) and the PKC(Boyle et al., 1991) pathways. As these pathways are also known regulators of AP-1 expression and activity, exploring how they affect AP-1 levels and dimerization during obesity is certainly an important challenge for future experiments. Moreover, extensive cross-talk between AP-1 and transcription factors of the NF-κB(Fujioka et al., 2004) and the nuclear receptor family(Glass and Saijo, 2010; Ricote and Glass, 2007; Wan et al., 2007) has been described. Future studies should reveal the molecular interplay of these pathways with AP-1 signaling in the context of NAFLD in both mice and human.

Experimental procedures

Animal procedures

Mice were maintained in a 12 hour light/12 hour dark cycle with food and water *ad libitum*. Chow (D8604, Harlan), 45% kCal/fat HFD (D12451, Research diets), 60%kCal/fat HFD (D12492, Research diets) were used as specified in the figure legends. If not indicated otherwise, male mice were used and HFD feeding was started between 4-8 weeks of age. Dox (1g/l) was supplied in sucrose-containing (100g/l) drinking water. The BXD mice were sacrificed after overnight fasting, while in other experiments, the mice were sacrificed in CO_2-chambers between 2pm and 5pm in the fed state. Fasted Cholesterol and TG measurements were performed using serum from overnight fasted mice. For intra-peritoneal glucose tolerance (GTT) and insulin tolerance tests(ITT), mice were fasted for 6 hours (GTT) or 8 hours (ITT) and intra-peritoneally injected with 1 mg glucose/kg body weight (GTT) or 0,5U Insulin/kg body weight (ITT). Glucose and insulin were diluted in PBS to an injectable volume. Blood glucose was determined by tail puncture for all time points. All mouse experiments were performed in accordance with local and institutional regulations. Details on mouse strains can be found in Table S1.

NIH-PA Author Manuscript

NIH-PA Author Manuscript

NIH-PA Author Manuscript

Blood analyses

Blood was collected from the submandibular vein, by tail puncture or by cardiac puncture at experimental endpoints. Unless indicated otherwise specified, parameters were analyzed in the fed state. Serum ALT, TG and cholesterol levels were determined using a Reflovet blood chemistry analyzer and glucose using an Accucheck glucose analyzer (Aviva). Serum Leptin, Resistin, Adiponectin and IL-6 were measured using Quantikine ELISA kits (R&D) and serum Insulin was determined with an ultrasensitive ELISA (Mercodia). Serum ß-HB and FFA were measured using enzymatic assays (Cayman Chemicals).

qRT-PCR/immunoblot analysis

qRT-PCR was performed using the GoTaq® qPCR Master Mix and an Eppendorf light cycler. Expression levels were calculated using the ΔCt-method. Data were normalized to a housekeeping gene (rps27 or rpl0). Primer sequences are available upon request. Immunoblot analysis was performed using standard protocols and following antibodies: ACC, PPARγ, CEBPβ, c-Jun, phospho-CREBP, total CREB (Cell Signaling), Vinculin (Sigma), PPARγ, Parp-1, CEBPα, c-Fos, Fra-1 (Santa Cruz), HNF4, FAS, Fabp1 (Abcam), and Fsp27 (Novus Biologicals), SREBP-1/2 (BD Bioscience). Nuclear extracts from liver tissue were obtained using the NE-PER Nuclear Protein Extraction Kit (Pierce).

Histology

H&E- and ORO-staining were performed using standard procedures. ORO-positive areas were quantified as previously described(Mehlem et al., 2013). IHC was performed as described (Hasenfuss et al., 2013) using following antibodies: PPARγ (Cell Signaling), CD45 (Abcam), F4/80 (AbD Serotec).

RNA microarray

RNA was isolated using the RNEasy Midi kit (Qiagen) and RNA integrity was evaluated using an Agilent 2100 Bioanalyzer. Samples of RNA integrity score above 7.8 were used for microarray analysis. 100ng of RNA was labeled with Cy3 (RNA pool from at least 5 control mice, which were either fed CD or HFD) or Cy5 (RNA samples from individual mutants, which were either fed CD or HFD) using the Low Input Quick Amp Labeling Kit Version 6.5 (Agilent). Labeled RNAs were purified using RNeasy spin columns (Qiagen) and hybridized to a mouse gene expression array G3 8×60K (Agilent microarray design ID 028005, P/N G4852A). On each array, the Cy3-labeled control pool and one Cy5 labeled mutant sample were hybridized at 65°C for 17 hours. The microarray was scanned on a 2505C DNA microarray scanner (Agilent) and images were analyzed using the Feature Extraction Software Version 10.7 (Agilent). Multiple testing correction was performed using the Benjamin-Hochberg procedure. Data are deposited in NCBI's Gene Expression Omnibus and are accessible through GEO Series accession number GSE52275 (http://www.ncbi.nlm.nih.gov/geo/query/acc.cgi?acc=GSE52275). Hepatic gene expression of the BXD strains was analyzed using Mouse Gene 1.0 ST Arrays (Affymetrix) and are accessible on http://www.genenetwork.org.Standard array analysis methods were used, e.g. RMA normalization, as described elsewhere(Irizarry et al., 2003).

NIH-PA Author Manuscript

NIH-PA Author Manuscript

NIH-PA Author Manuscript

Gene pathway analysis

Microarray data were analyzed separately in CD and HFD conditions by comparing control to mutant livers. All nominally significant changes with fold change ≥ 1.5 were retained. Gene sets were then winnowed using multiple testing correction (Benjamin-Hochberg) and entered independently into Web Gestalt (http://bioinfo.vanderbilt.edu/webgestalt/). Enriched pathways were generated based on KEGG gene ontology annotations. The PPARγ signaling pathway was found significantly modulated in both dietary conditions. The two independently-generated pathways were then overlaid and redrawn to generate the pathway diagram.

Cell culture and reporter assay

HuH7 and 293T cells were cultured in DMEM/10%FCS at 37°C and 5% CO_2. For reporter assays, 0.8×10^5 HuH7 or 293T cells were plated per well of a 24-well plate. 24 hours later, 0.01μg Renilla vector, 0.2μg *PPARG2*-luc vector(Saladin et al., 1999)and 0.6μg pCMV-AP-1 or pCMV-empty control vector were transfected using Lipofectamine 2000 (Invitrogen). Cells were harvested 48h after transfection and luciferase activity was analyzed using the Dual-Glo Luciferase Assay (Promega).

Liver TG content analysis

Frozen liver tissue (25-75mg) was homogenized in chloroform/methanol (8:1 v/v; 500ul per 25 mg tissue) and shaken at RT for 8-16 hours. H_2SO_4 was added to a final concentration of 0.28M. After centrifugation, the lower phase was collected, dried, and TG content was measured using an enzymatic assay (Caymen Chem).

Chromatin immunoprecipitation (ChIP)

ChIP was performedusing following antibodies: Flag (F3165, Sigma), Fra-1 (SC-183, Santa Cruz), Fra-2 (rat, CNIO polyclonal), c-Fos (PC-05, Calbiochem), c-Jun (BD), JunB (SC-73, Santa Cruz), JunD (CS5000, Cell Signaling). Pan Jun ChIP with HuH7 cells has been performed with a mixture of2 antibodies raised against an epitope present in all Jun proteins. For details on the ChIP protocol, see also Supplementary Experimental Procedures.

Statistical analysis

Statistical significance was calculated using Student's two-tailed t-test if not indicated otherwise, *: $p<0.05$; **: $p<0.01$; ***: $p<0.001$, ****: $p<0.0001$.

Supplementary Material

Refer to Web version on PubMed Central for supplementary material.

Acknowledgments

We thank Drs. N. Djouder, M. Perez-Moreno, R. Ricci, M. Serrano and G. Sumara for critical reading of the manuscript and valuable suggestions; the CNIO Transgenics Unit and G. Luque and G. Medrano for technical help with mouse procedures. J.A. is the Nestlé Chair in Energy Metabolism and his laboratory is supported by grants from the Ecole Polytechnique Fédérale de Lausanne, the EU Ideas program (AdG-231138), the Swiss National Science Foundation (31003A-140780) and NIH (R01AG043930). Erwin F. Wagner laboratory is supported by the

NIH-PA Author Manuscript

NIH-PA Author Manuscript

NIH-PA Author Manuscript

Banco Bilbao Vizcaya Argentaria Foundation (F-BBVA), a grant from the Spanish Ministry of Economy (BFU2012-40230) and an ERC-Advanced grant ERC-FCK/2008/37. Martin K. Thomsen was supported by a Juan de la Cierva postdoctoral fellowship. Sebastian C. Hasenfuss received a Boehringer Ingelheim Fonds (BIF) PhD fellowship and an EMBO short term fellowship (ASTF 198–2012).

References

Bakiri L, Matsuo K, Wisniewska M, Wagner EF, Yaniv M. Promoter specificity and biological activity of tethered AP-1 dimers. Mol Cell Biol. 2002; 22:4952–4964. [PubMed: 12052899]

Bakiri L, Wagner EF. Mouse models for liver cancer. Molecular oncology. 2013; 7:206–223. [PubMed: 23428636]

Behrens A, Sibilia M, David JP, Mohle-Steinlein U, Tronche F, Schutz G, Wagner EF. Impaired postnatal hepatocyte proliferation and liver regeneration in mice lacking c-jun in the liver. EMBO J. 2002; 21:1782–1790. [PubMed: 11927562]

Boyle WJ, Smeal T, Defize LH, Angel P, Woodgett JR, Karin M, Hunter T. Activation of protein kinase C decreases phosphorylation of c-Jun at sites that negatively regulate its DNA-binding activity. Cell. 1991; 64:573–584. [PubMed: 1846781]

Browning JD, Horton JD. Molecular mediators of hepatic steatosis and liver injury. J Clin Invest. 2004; 114:147–152. [PubMed: 15254578]

Chang BH, Li L, Paul A, Taniguchi S, Nannegari V, Heird WC, Chan L. Protection against fatty liver but normal adipogenesis in mice lacking adipose differentiation-related protein. Mol Cell Biol. 2006; 26:1063–1076. [PubMed: 16428458]

Cohen JC, Horton JD, Hobbs HH. Human fatty liver disease: old questions and new insights. Science. 2011; 332:1519–1523. [PubMed: 21700865]

Dalen KT, Schoonjans K, Ulven SM, Weedon-Fekjaer MS, Bentzen TG, Koutnikova H, Auwerx J, Nebb HI. Adipose tissue expression of the lipid droplet-associating proteins S3-12 and perilipin is controlled by peroxisome proliferator-activated receptor-gamma. Diabetes. 2004; 53:1243–1252. [PubMed: 15111493]

Eferl R, Ricci R, Kenner L, Zenz R, David JP, Rath M, Wagner EF. Liver tumor development. c-Jun antagonizes the proapoptotic activity of p53. Cell. 2003; 112:181–192. [PubMed: 12553907]

Eferl R, Wagner EF. AP-1: a double-edged sword in tumorigenesis. Nat Rev Cancer. 2003; 3:859–868. [PubMed: 14668816]

Farese RV Jr. Zechner R, Newgard CB, Walther TC. The problem of establishing relationships between hepatic steatosis and hepatic insulin resistance. Cell Metab. 2012; 15:570–573. [PubMed: 22560209]

Feng D, Liu T, Sun Z, Bugge A, Mullican SE, Alenghat T, Liu XS, Lazar MA. A circadian rhythm orchestrated by histone deacetylase 3 controls hepatic lipid metabolism. Science. 2011; 331:1315–1319. [PubMed: 21393543]

Fleischmann A, Hafezi F, Elliott C, Reme CE, Ruther U, Wagner EF. Fra-1 replaces c-Fos-dependent functions in mice. Genes Dev. 2000; 14:2695–2700. [PubMed: 11069886]

Fuest M, Willim K, MacNelly S, Fellner N, Resch GP, Blum HE, Hasselblatt P. The transcription factor c-Jun protects against sustained hepatic endoplasmic reticulum stress thereby promoting hepatocyte survival. Hepatology. 2012; 55:408–418. [PubMed: 21953113]

Fujimoto T, Ohsaki Y, Cheng J, Suzuki M, Shinohara Y. Lipid droplets: a classic organelle with new outfits. Histochem Cell Biol. 2008; 130:263–279. [PubMed: 18546013]

Fujioka S, Niu J, Schmidt C, Sclabas GM, Peng B, Uwagawa T, Li Z, Evans DB, Abbruzzese JL, Chiao PJ. NF-kappaB and AP-1 connection: mechanism of NF-kappaB-dependent regulation of AP-1 activity. Mol Cell Biol. 2004; 24:7806–7819. [PubMed: 15314185]

Gavrilova O, Haluzik M, Matsusue K, Cutson JJ, Johnson L, Dietz KR, Nicol CJ, Vinson C, Gonzalez FJ, Reitman ML. Liver peroxisome proliferator-activated receptor gamma contributes to hepatic steatosis, triglyceride clearance, and regulation of body fat mass. J Biol Chem. 2003; 278:34268–34276. [PubMed: 12805374]

Glass CK, Saijo K. Nuclear receptor transrepression pathways that regulate inflammation in macrophages and T cells. Nat Rev Immunol. 2010; 10:365–376. [PubMed: 20414208]

NIH-PA Author Manuscript

NIH-PA Author Manuscript

NIH-PA Author Manuscript

Halazonetis TD, Georgopoulos K, Greenberg ME, Leder P. c-Jun dimerizes with itself and with c-Fos, forming complexes of different DNA binding affinities. Cell. 1988; 55:917–924. [PubMed: 3142692]

Hasenfuss SC, Bakiri L, Thomsen MK, Hamacher R, Wagner EF. The AP-1 transcription factor Fra-1 is dispensable for murine liver fibrosis, but modulates xenobiotic metabolism. Hepatology. 2013 doi: 10.1002/hep.26518.

Hasselblatt P, Rath M, Komnenovic V, Zatloukal K, Wagner EF. Hepatocyte survival in acute hepatitis is due to c-Jun/AP-1-dependent expression of inducible nitric oxide synthase. Proc Natl Acad Sci U S A. 2007; 104:17105–17110. [PubMed: 17940019]

Hess J, Angel P, Schorpp-Kistner M. AP-1 subunits: quarrel and harmony among siblings. J Cell Sci. 2004; 117:5965–5973. [PubMed: 15564374]

Hibi M, Lin A, Smeal T, Minden A, Karin M. Identification of an oncoprotein- and UV-responsive protein kinase that binds and potentiates the c-Jun activation domain. Genes Dev. 1993; 7:2135–2148. [PubMed: 8224842]

Huang da W, Sherman BT, Lempicki RA. Systematic and integrative analysis of large gene lists using DAVID bioinformatics resources. Nature protocols. 2009; 4:44–57.

Irizarry RA, Hobbs B, Collin F, Beazer-Barclay YD, Antonellis KJ, Scherf U, Speed TP. Exploration, normalization, and summaries of high density oligonucleotide array probe level data. Biostatistics. 2003; 4:249–264. [PubMed: 12925520]

Kanehisa M, Goto S, Sato Y, Furumichi M, Tanabe M. KEGG for integration and interpretation of large-scale molecular data sets. Nucleic Acids Res. 2012; 40:D109–114. [PubMed: 22080510]

Kim HI, Koh YK, Kim TH, Kwon SK, Im SS, Choi HS, Kim KS, Ahn YH. Transcriptional activation of SHP by PPAR-gamma in liver. Biochemical and biophysical research communications. 2007; 360:301–306. [PubMed: 17601490]

Kim SC, Kim C, Axe D, Cook A, Lee M, Li T, Smallwood N, Chiang JY, Hardwick JP, Moore DD, et al. All-trans-retinoic acid ameliorates hepatic steatosis in mice via a novel transcriptional cascade. Hepatology. 2013 doi: 10.1002/hep.26699.

Kim SJ, Kahn CR. Insulin stimulates phosphorylation of c-Jun, c-Fos, and Fos-related proteins in cultured adipocytes. J Biol Chem. 1994; 269:11887–11892. [PubMed: 7512956]

Knutson SK, Chyla BJ, Amann JM, Bhaskara S, Huppert SS, Hiebert SW. Liver-specific deletion of histone deacetylase 3 disrupts metabolic transcriptional networks. EMBO J. 2008; 27:1017–1028. [PubMed: 18354499]

Lara-Castro C, Garvey WT. Intracellular lipid accumulation in liver and muscle and the insulin resistance syndrome. Endocrinol Metab Clin North Am. 2008; 37:841–856. [PubMed: 19026935]

Lazo M, Clark JM. The epidemiology of nonalcoholic fatty liver disease: a global perspective. Semin Liver Dis. 2008; 28:339–350. [PubMed: 18956290]

Lee YJ, Ko EH, Kim JE, Kim E, Lee H, Choi H, Yu JH, Kim HJ, Seong JK, Kim KS, et al. Nuclear receptor PPAR gamma-regulated monoacylglycerol O-acyltransferase 1 (MGAT1) expression is responsible for the lipid accumulation in diet-induced hepatic steatosis. Proc Natl Acad Sci U S A. 2012; 109:13656–13661. [PubMed: 22869740]

Machida K, Tsukamoto H, Liu JC, Han YP, Govindarajan S, Lai MM, Akira S, Ou JH. c-Jun mediates hepatitis C virus hepatocarcinogenesis through signal transducer and activator of transcription 3 and nitric oxide-dependent impairment of oxidative DNA repair. Hepatology. 2010; 52:480–492. [PubMed: 20683948]

Matsuo K, Owens JM, Tonko M, Elliott C, Chambers TJ, Wagner EF. Fosl1 is a transcriptional target of c-Fos during osteoclast differentiation. Nat Genet. 2000; 24:184–187. [PubMed: 10655067]

Matsusue K, Haluzik M, Lambert G, Yim SH, Gavrilova O, Ward JM, Brewer B Jr. Reitman ML, Gonzalez FJ. Liver-specific disruption of PPAR gamma in leptin-deficient mice improves fatty liver but aggravates diabetic phenotypes. J Clin Invest. 2003; 111:737–747. [PubMed: 12618528]

Matsusue K, Kusakabe T, Noguchi T, Takiguchi S, Suzuki T, Yamano S, Gonzalez FJ. Hepatic steatosis in leptin-deficient mice is promoted by the PPAR gamma target gene Fsp27. Cell Metab. 2008; 7:302–311. [PubMed: 18396136]

Medina-Gomez G, Gray SL, Yetukuri L, Shimomura K, Virtue S, Campbell M, Curtis RK, Jimenez-Linan M, Blount M, Yeo GS, et al. PPAR gamma 2 prevents lipotoxicity by controlling adipose

NIH-PA Author Manuscript

NIH-PA Author Manuscript

NIH-PA Author Manuscript

tissue expandability and peripheral lipid metabolism. PLoS Genet. 2007; 3:e64. [PubMed: 17465682]

Mehlem A, Hagberg CE, Muhl L, Eriksson U, Falkevall A. Imaging of neutral lipids by oil red O for analyzing the metabolic status in health and disease. Nature protocols. 2013; 8:1149–1154.

Min L, Ji Y, Bakiri L, Qiu Z, Cen J, Chen X, Chen L, Scheuch H, Zheng H, Qin L, et al. Liver cancer initiation is controlled by AP-1 through SIRT6-dependent inhibition of survivin. Nat Cell Biol. 2012; 14:1203–1211. [PubMed: 23041974]

Moran-Salvador E, Lopez-Parra M, Garcia-Alonso V, Titos E, Martinez-Clemente M, Gonzalez-Periz A, Lopez-Vicario C, Barak Y, Arroyo V, Claria J. Role for PPAR gamma in obesity-induced hepatic steatosis as determined by hepatocyte- and macrophage-specific conditional knockouts. FASEB J. 2011; 25:2538–2550. [PubMed: 21507897]

Newberry EP, Xie Y, Kennedy S, Han X, Buhman KK, Luo J, Gross RW, Davidson NO. Decreased hepatic triglyceride accumulation and altered fatty acid uptake in mice with deletion of the liver fatty acid-binding protein gene. J Biol Chem. 2003; 278:51664–51672. [PubMed: 14534295]

Newberry EP, Xie Y, Kennedy SM, Luo J, Davidson NO. Protection against Western diet-induced obesity and hepatic steatosis in liver fatty acid-binding protein knockout mice. Hepatology. 2006; 44:1191–1205. [PubMed: 17058218]

Peirce JL, Lu L, Gu J, Silver LM, Williams RW. A new set of BXD recombinant inbred lines from advanced intercross populations in mice. BMC Genet. 2004; 5:7. [PubMed: 15117419]

Puri V, Ranjit S, Konda S, Nicoloro SM, Straubhaar J, Chawla A, Chouinard M, Lin C, Burkart A, Corvera S, et al. Cidea is associated with lipid droplets and insulin sensitivity in humans. Proc Natl Acad Sci U S A. 2008; 105:7833–7838. [PubMed: 18509062]

Purushotham A, Schug TT, Xu Q, Surapureddi S, Guo X, Li X. Hepatocyte-specific deletion of SIRT1 alters fatty acid metabolism and results in hepatic steatosis and inflammation. Cell Metab. 2009; 9:327–338. [PubMed: 19356714]

Ricote M, Glass CK. PPARs and molecular mechanisms of transrepression. Biochim Biophys Acta. 2007; 1771:926–935. [PubMed: 17433773]

Saladin R, Fajas L, Dana S, Halvorsen YD, Auwerx J, Briggs M. Differential regulation of peroxisome proliferator activated receptor gamma1 (PPAR gamma1) and PPAR gamma2 messenger RNA expression in the early stages of adipogenesis. Cell Growth Differ. 1999; 10:43–48. [PubMed: 9950217]

Sethi JK, Vidal-Puig AJ. Thematic review series: adipocyte biology. Adipose tissue function and plasticity orchestrate nutritional adaptation. J Lipid Res. 2007; 48:1253–1262.

Shaulian E, Karin M. AP-1 as a regulator of cell life and death. Nat Cell Biol. 2002; 4:131–136.

Smedile A, Bugianesi E. Steatosis and hepatocellular carcinoma risk. Eur Rev Med Pharmacol Sci. 2005; 9:291–293. [PubMed: 16231592]

Sun Z, Miller RA, Patel RT, Chen J, Dhir R, Wang H, Zhang D, Graham MJ, Unterman TG, Shulman GI, et al. Hepatic Hdac3 promotes gluconeogenesis by repressing lipid synthesis and sequestration. Nat Med. 2012; 18:934–942. [PubMed: 22561686]

Thepot D, Weitzman JB, Barra J, Segretain D, Stinnakre MG, Babinet C, Yaniv M. Targeted disruption of the murine junD gene results in multiple defects in male reproductive function. Development. 2000; 127:143–153. [PubMed: 10654608]

Tontonoz P, Spiegelman BM. Fat and beyond: the diverse biology of PPAR gamma. Annu Rev Biochem. 2008; 77:289–312. [PubMed: 18518822]

Varela GM, Antwi DA, Dhir R, Yin X, Singhal NS, Graham MJ, Crooke RM, Ahima RS. Inhibition of ADRP prevents diet-induced insulin resistance. Am J Physiol Gastrointest Liver Physiol. 2008; 295:G621–628. [PubMed: 18669627]

Verde P, Casalino L, Talotta F, Yaniv M, Weitzman JB. Deciphering AP-1 function in tumorigenesis: fra-ternizing on target promoters. Cell Cycle. 2007; 6:2633–2639. [PubMed: 17957143]

Wagner EF, Nebreda AR. Signal integration by JNK and p38 MAPK pathways in cancer development. Nat Rev Cancer. 2009; 9:537–549. [PubMed: 19629069]

Wagner EF, Schonthaler HB, Guinea-Viniegra J, Tschachler E. Psoriasis: what we have learned from mouse models. Nat Rev Rheumatol. 2010; 6:704–714. [PubMed: 20877306]

NIH-PA Author Manuscript

NIH-PA Author Manuscript

NIH-PA Author Manuscript

Wan Y, Chong LW, Evans RM. PPAR-gamma regulates osteoclastogenesis in mice. Nat Med. 2007; 13:1496–1503. [PubMed: 18059282]

Zhou L, Xu L, Ye J, Li D, Wang W, Li X, Wu L, Wang H, Guan F, Li P. Cidea promotes hepatic steatosis by sensing dietary fatty acids. Hepatology. 2012; 56:95–107. [PubMed: 22278400]

NIH-PA Author Manuscript

NIH-PA Author Manuscript

NIH-PA Author Manuscript

Highlights

- AP-1 is a regulator of hepatic lipid metabolism.

- Fra-1prevents and importantly, fully reverts NAFLD *in vivo*.

- c-Fos/c-Jun dimers activate, while Fra/c-Jun dimers repress the *Pparg2* promoter.

-*JunD* deficiency impairs PPARγ signaling and inhibits NAFLD.

NIH-PA Author Manuscript

NIH-PA Author Manuscript

NIH-PA Author Manuscript

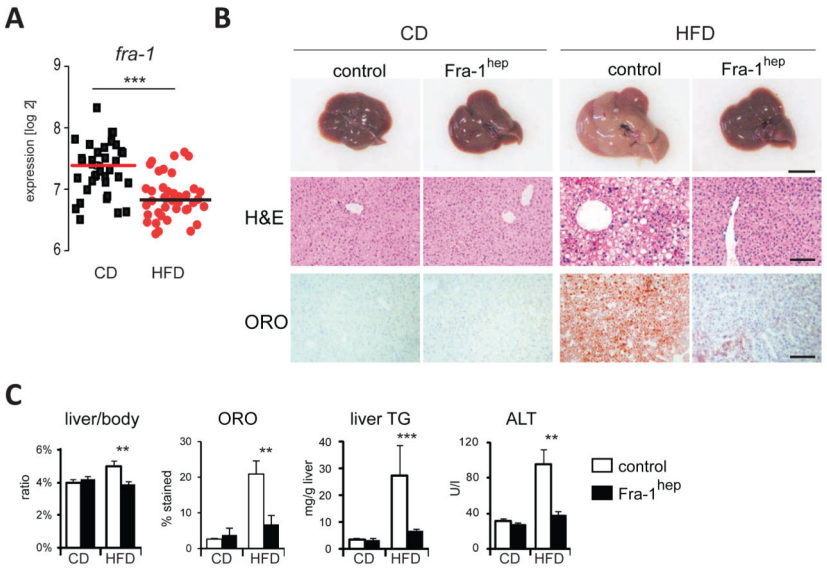

Figure 1. Fra-1 is regulated by HFD and inhibits NAFLD and PPARγ expression

(A) Hepatic *fra-1* expression in CD and HFD (for 5 months; 60% kCal/fat) in 42 BXD inbred strains. Each data point represents the mean expression of 5 mice. **(B,C)**, Fra-1^{hep} mice and control littermates were on CD or HFD (for 5-9 months; 45% kCal/fat); n≥5/cohort. **(B)** Representative liver pictures and histology in Fra-1^{hep} and control mice; ORO=Oil-RedO; bars=1cm and 100μm. **(C)** Quantitation of ORO-positive areas, liver/body ratio, liver TG content and serum ALT levels. Bar graphs are presented as mean±SEM. See also Figure S1 and Table S2 A,B.

NIH-PA Author Manuscript

NIH-PA Author Manuscript

NIH-PA Author Manuscript

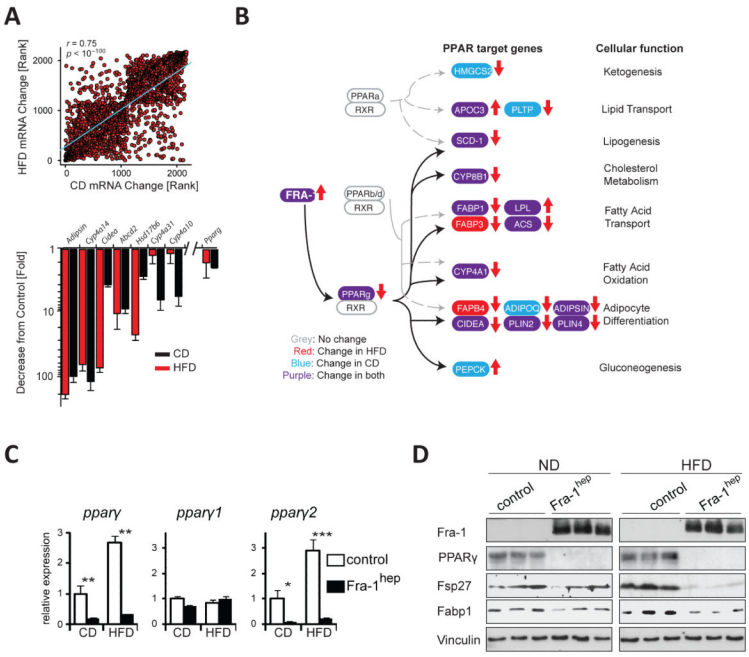

Figure 2. Fra-1 regulates the PPARγ pathway

(A-D) Fra-1^{hep} mice and control littermates on CD or HFD (for 5-9 months; 45 % kCal/fat); n≥5/condition. **(A)** Top: Spearman correlation of ≥1.5 fold-changed hepatic transcripts in Fra-1^{hep} and control littermates (C57BL/6J) in CD (x-axis) and HFD (y-axis). Bottom: Top common downregulated genes in Fra-1^{hep} livers. **(B)** KEGG pathway analyses for the top 2000 most changed transcripts: PPAR target genes and their cellular functions are indicated. Transcripts changed in CD, HFD or both are highlighted in blue, red and purple respectively. Arrows indicate up- or down-regulation. **(C)** qRT-PCR analyses of *pparγ* and its isoforms. **(D)**Immunoblot analyses in Fra-1^{hep} and control mice. Vinculin served as loading control. Bar graphs are presented as mean±SEM. See also Figure S2 and Table S3.

NIH-PA Author Manuscript
NIH-PA Author Manuscript
NIH-PA Author Manuscript

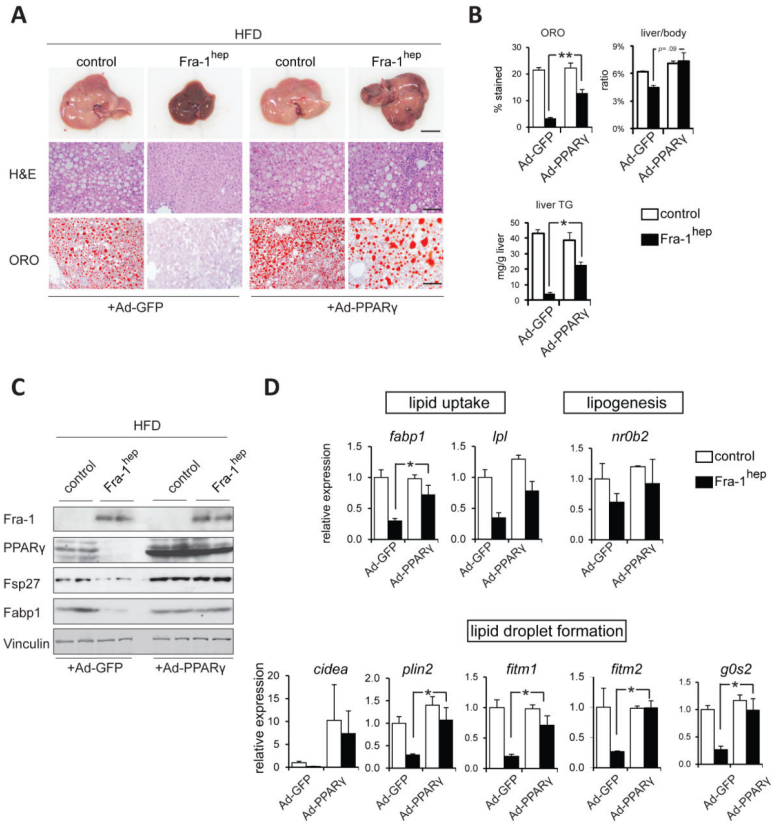

Figure 3. PPARγ delivery restores NAFLD development in Fra-1^{hep} mice

(A-D) Fra-1^{hep} and control littermates on HFD (for 4-5 months, 45 % kCal/fat) were injected with Adenoviruses expressing PPARγ (Ad-PPARγ) or GFP (Ad-GFP) 8-10 days prior to sacrifice. n=3 for control genotype/cohort; n=4 for Fra-1^{hep} mice/cohort. **(A)** Liver macroscopy and histology; bars=1cm and 100μm. **(B)**Quantitation of ORO-positive areas, liver/body ratio and liver TG. **(C)**Immunoblot analyses in Fra-1^{hep} and control mice. Vinculin served as loading control.**(D)** qRT-PCR analyses of PPARγ target genes involved in lipid uptake and lipid droplet formation; Ad-GFP controls are set to 1. Bar graphs are presented as mean±SEM.

NIH-PA Author Manuscript

NIH-PA Author Manuscript

NIH-PA Author Manuscript

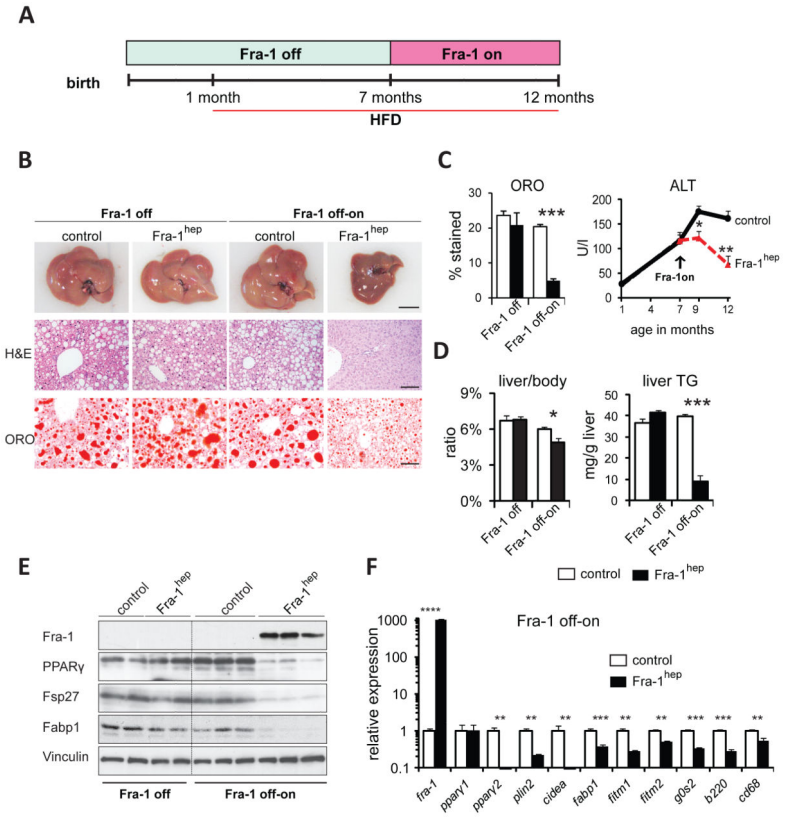

Figure 4. Fra-1 expression reverts NAFLD and liver damage

(A) Fra-1^{hep} and control littermates were maintained in the "Fra-1 off" state and HFD (45 % kCal/fat) was supplied from 1 month of age. Mice were analyzed at 7 months (Fra-1 off, n=2/cohort) or kept on HFD until 12 months, while transgene expression was induced (Fra-1 off-on, n=6/cohort). **(B)**Liver macroscopy and histology; bars=1cm and 100μm. **(C)** Serum ALT. **(D)**Quantitation of ORO-positive areas, liver/body ratio and liver TG content. **(E)**Immunoblot analyses in Fra-1^{hep} and control mice. Vinculin served as loading control. **(F)** qRT-PCR analyses of *fra-1*, *pparγ* isoforms, PPARγ target genes and inflammation markers (Fra-1 off-on). Bar graphs are presented as mean±SEM.

NIH-PA Author Manuscript
NIH-PA Author Manuscript
NIH-PA Author Manuscript

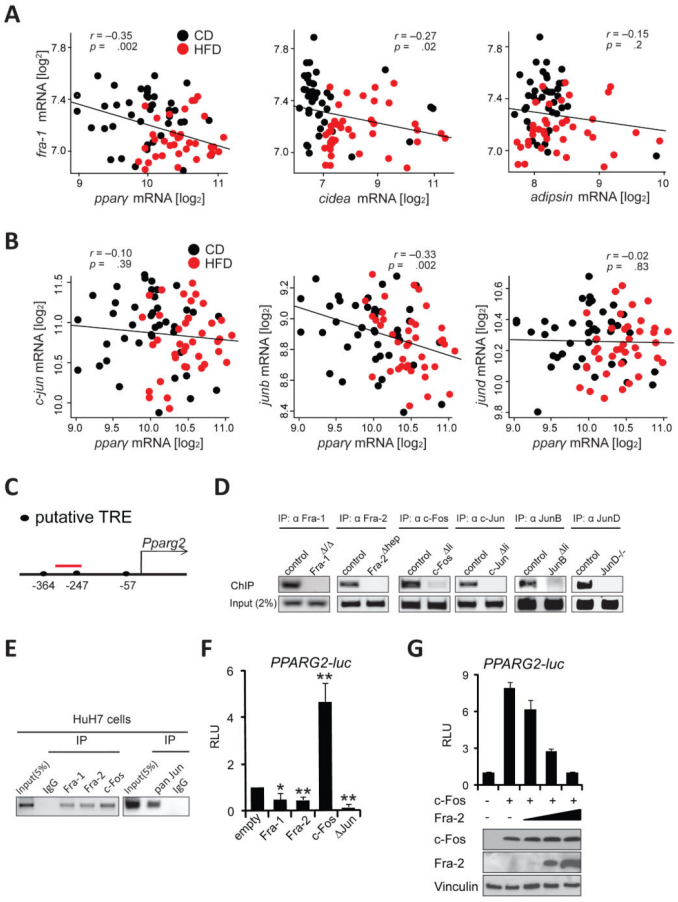

Figure 5. Several AP-1 proteins regulate the PPARγ pathway

Correlation plots for *fra-1* with *pparγ*,*cidea* and *adipsin* **(A)** and for *Jun* members with *pparγ* **(B)** in CD and HFD (5months; 60 % kCal/fat) in the BXD inbred family. Each data point represents the average expression from 5 pooled mice. Pearson's r was used to analyze correlations and *p*-values are indicated. **(C)** Proximal murine *Pparg2* promoter: Position of the putative AP-1 binding TPA-responsive element (TRE) is indicated relative to the transcription start. The ChIP-PCR amplicon is depicted in red. **(D)**ChIP assays using hepatic chromatin from AP-1-deficient mice. Endpoint PCR products representative of 3 independent experiments are shown. **(E)** ChIP assays in Huh7 cells; primers amplifying a region homologous to **(C)** were used. Data are representative of 3 independent experiments. **(F,G)** Human *PPARG2* reporter assays in HuH7 cells. Data are mean±s.e.m of 4 independent experiments in **(F)**. Technical replicates of one representative experiment (n=2) is shown and ectopic c-Fos and Fra-2 expression is confirmed by immunoblot in **(G)**. RLU: relative luminescence units. ΔJun: truncated c-Jun. Control (empty vector) is set to 1. Bar graphs are presented as mean±SEM. See also Figure S3.

NIH-PA Author Manuscript
NIH-PA Author Manuscript
NIH-PA Author Manuscript

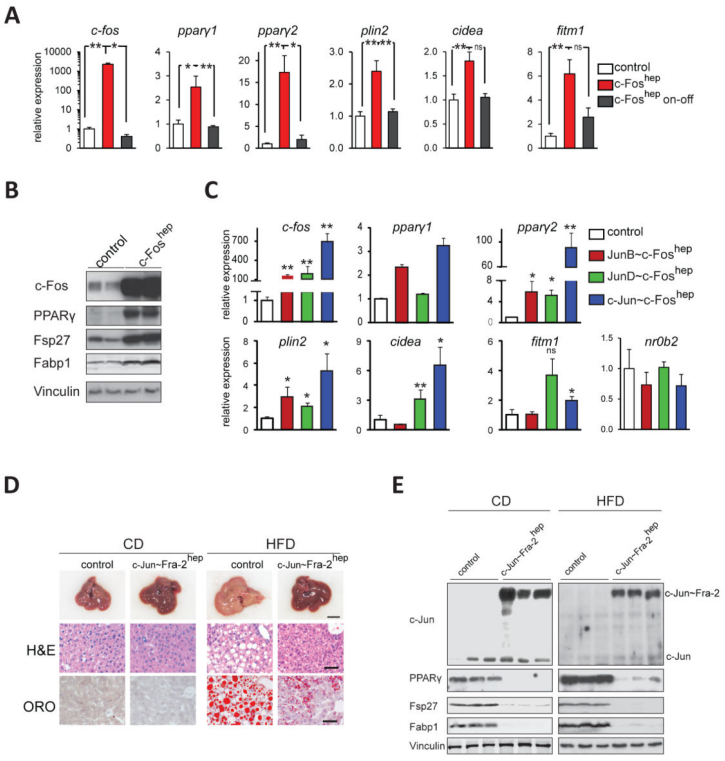

Figure6. Antagonistic regulation of PPARγ signaling by AP-1

(A) qRT-PCR analyses of *c-fos* (endogenous+ectopic), *ppar γ1/2* and PPARγ targets in c-Fos^{hep} and control mice. c-Fos expression was induced for 1 week (c-Fos on) or induced for 1 week and switched off for 1 week (c-Fos on-off). n=8 for c-Fos^{hep}mice (on), n=10 for controls (on), n=3 for c-Fos^{hep} (on-off). **(B)** Immunoblot analyses in c-Fos^{hep} (c-Fos on for 1 week) and control mice. Vinculin served as a loading control. Blots are representative of 3 controls and 4 mutants.**(C)**qRT-PCR analyses in JunB~c-Fos^{hep}(n=6), JunD~c-Fos^{hep}(n=5), and c-Jun~c-Fos^{hep}(n=4)(transgene on for 1 month) and control (n=5) mice. Liver macroscopy and histology **(D)** and immunoblot analyses **(E)** of c-Jun~Fra-2^{hep} mice (c-Jun~Fra-2 switched on at 1 month) and control littermates on CD or HFD (for 4 months;60 % kCal/fat). Vinculin served as loading control; n≥5/condition. Bar graphs are presented as mean±SEM. See also Figure S4.

NIH-PA Author Manuscript

NIH-PA Author Manuscript

NIH-PA Author Manuscript

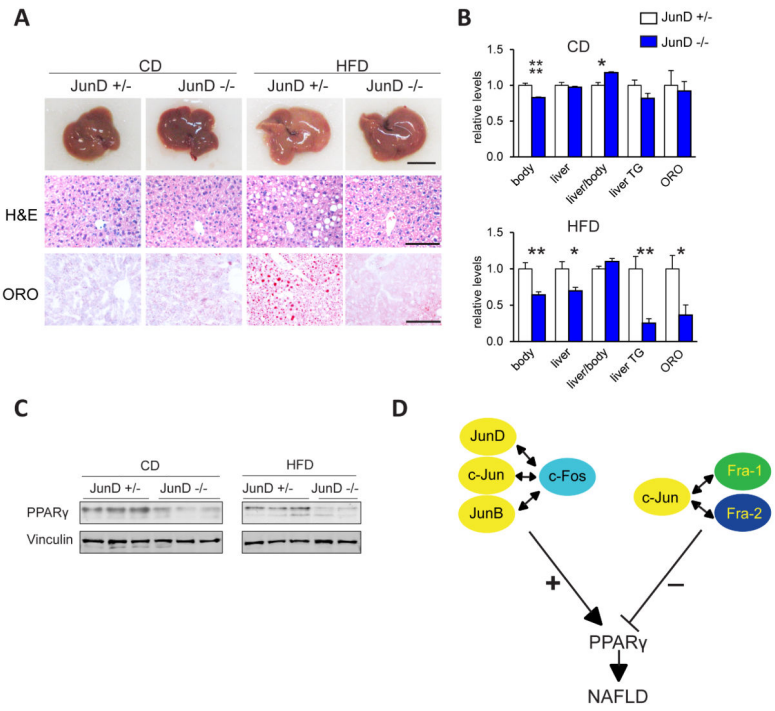

Figure7. JunD is essential for PPARγ expression and steatosis formation

(A-C) Analyses of JunD$^{-/-}$ and JunD$^{+/-}$ control littermates (males and females) on CD or HFD (for 9 months; 45 % kCal/fat); n≥7/condition. **(A)** Representative liver macroscopy and histology; bars=1cm and 100μm. **(B)** Macroscopic parameters, serum ALT, liver TG content and quantitation of ORO-positive areas; relative levels are plotted and sex matched controls set to 1. Bar graphs are presented as mean±SEM. **(C)**Immunoblot analysis for PPARγ and Vinculin.**(D)** Antagonistic regulation of PPARγ expression by different AP-1 dimers: c-Fos induces PPARγ as a dimer with any Jun protein, while Fra-1 and Fra-2 repress PPARγ, likely by dimerizing with c-Jun, thereby affecting hepatic lipid metabolism and NAFLD. See also Figure S5 and Table S4.